Exciton spectra in two-dimensional graphene derivatives

Shouting Huang, Yufeng Liang, and Li Yang
Department of Physics, Washington University in St. Louis, St. Louis, Missouri 63136, USA
(Received 28 January 2013; revised manuscript received 21 July 2013; published 30 August 2013)

The energy spectra and wave functions of bound excitons in important two-dimensional (2D) graphene derivatives, i.e., graphyne and graphane, are found to be strongly modified by quantum confinement, making them qualitatively different from the usual Rydberg series. However, their parity and optical selection rules are preserved. Thus a one-parameter modified hydrogenic model is applied to quantitatively explain the *ab initio* exciton spectra, and allows one to extrapolate the electron-hole binding energy from optical spectroscopies of 2D semiconductors without costly simulations. Meanwhile, our calculated optical absorption spectrum and enhanced spin singlet-triplet splitting project graphyne, an allotrope of graphene, as a candidate for intriguing energy and biomedical applications.

DOI: 10.1103/PhysRevB.88.075441 PACS number(s): 71.35.Cc, 78.67.−n, 81.05.ue

I. INTRODUCTION

Exciton spectrum, the sequence of electron-hole (*e-h*) binding energies, is the most direct way to understand excitonic effects of semiconductors. It is also the foundation for constructing useful models widely used to identify excitonic effects in optical spectroscopy experiments. For example, the *e-h* binding energy can be conveniently extrapolated from the measured sequence of exciton peaks according to model predictions. In particular, *e-h* interactions are known to be dramatically enhanced in reduced dimensional structures.[1–6] Other than the change of optical spectroscopies, how these unique quantum confinements influence exciton spectra and how one subsequently modifies corresponding *e-h* models have been of fundamental interest. As a result, based on the knowledge of exciton spectra, numerous exciton models of one-dimensional (1D) nanostructures[7–9] and quantum wells[10–14] have been proposed, which explain experimental results without costly simulations.

Recently many-electron effects and optical properties of graphene and its derivatives have ignited substantial interests because of their unique many-electron effects.[15–18] Because the thickness of these 2D structures is only a few angstroms, the perpendicular confinement is extremely strong, making previous models based on quantum wells (usually with a thickness of tens of nanometers) inappropriate for these 2D structures. More importantly, other than studies of the optical absorption, the exciton spectra of these novel materials are largely unknown. Therefore, we are unable to extract the general features of *e-h* interactions and build appropriate exciton models in these confined 2D systems.

The first-principles simulation based on the many-body perturbation theory (MBPT) is particularly useful to solve the above problems because this reliable calculation can provide the binding energy spectrum of excitons (including dark and bright states), optical activities, and even their wave functions, at the quantum-mechanical level. This motivates us to employ this method to calculate excitonic effects in important derivatives of graphene, i.e., graphyne[19–24] and graphane.[18,25–28] First, we expect to reveal the unknown exciton spectra of these novel 2D structures; secondly, we will build a quantitative model for identifying excitonic effects of more general 2D semiconductors without costly *ab initio* simulations, e.g., extrapolating the *e-h* binding energy, which is hard to measure directly in experiments.

Beyond fundamental scientific motivations, graphyne, a novel allotrope of graphene, is of particular interest for optical applications. Unlike other graphene derivatives, such as graphane and fluorographene, whose low-energy optical transitions are depressed by the tetrahedral symmetry,[15] the low-energy optical activity of graphyne may be prominent because of its planar atomistic structure and corresponding active transitions between π electronic states.[29] Particularly large-scale graphyne has not been fabricated to date despite substantial synthesis advances.[29–35] A quantitative prediction of electric and optical properties of graphyne is crucial to foresee potential applications and motivate more research efforts.

In this paper, we begin by revealing excited-state properties of a graphyne structure of current fabrication interest. The quasiparticle (QP) band gap is appreciable (1.4 eV); the lowest-energy optical absorption peak is located at 1.0 eV, meaning a 400-meV *e-h* binding energy; the near-infrared optical absorbance is more than 6%, making our studied graphyne one of the most efficient optical absorbers among known materials; this graphyne structure possesses an impressive spin singlet-triplet splitting ($\sim$150 meV) of excitons. These features promise exciting energy and biomedical applications.

Moreover, based on our calculated exciton spectrum, we propose a modified one-parameter hydrogenic model, in which the Coulomb potential is revised to capture the anisotropic quantum confinement and *e-h* exchange interactions of such a 2D semiconductor. To justify this model, we have applied it to graphyne and graphane, achieving excitonic spectra consistent with *ab initio* results. Therefore, this model may provide a convenient way to estimate the exciton binding energy without knowledge of the QP band gap, which shall be of broad interest to identify many-electron effects from the optical spectroscopy of 2D nanostructures.

The remainder of this paper is organized as follows: in Sec. II, we introduce the computing approaches and calculation details; in Sec. III, quasiparticle band gaps and excitonic effects on the optical absorption spectrum of graphyne are presented; in Sec. IV, we present the exciton spectrum of graphyne; in Sec. V, the modified hydrogenic model is proposed to describe

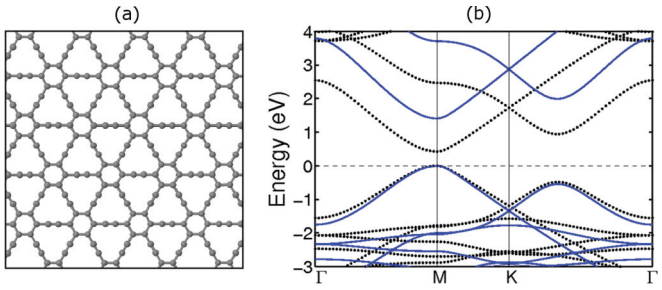

FIG. 1. (Color online) (a) Top view of the ball-stick model of our studied graphyne structure. (b) DFT and QP electronic band structures. The black dots represent the DFT result and the blue curves are the QP band structure. The top of valence band from both calculations is always set to be zero.

excitons in 2D semiconductors; in Sec. VI, the proposed model is applied to explain the exciton spectrum of graphane; in Sec. VII, we further discuss our exciton model and included many-electron effects; in Sec. VIII, we summarize our studies and conclusion.

II. COMPUTING SETUP

The studied graphyne structure is shown in Fig. 1(a), which is predicted by previous studies to be a direct-gap semiconductor,[24] a signature for intriguing optical properties. The ground state is obtained by density functional theory (DFT)/local density approximation (LDA). The calculations are done in a plane-wave basis using normconserving pseudopotentials with a 60 Ry energy cutoff. A coarse $16 \times 16 \times 1k$-point grid of the first Brillouin zone (BZ) is employed to compute the self-energy within the single-shot G_0W_0 approximation[36] with a layered Coulomb truncation. A fine k-grid ($64 \times 64 \times 1$) is interpolated from the coarse grid ($16 \times 16 \times 1$) to obtain the converged excitonic states and optical absorption spectrum by solving the Bethe-Salpeter equation (BSE).[37] Four valence bands and four conduction bands are included to calculate optical absorption spectra of the incident light polarized parallel to the graphyne plane because of the depolarization effect.[1,6]

III. QUASIPARTICLE ENERGY AND OPTICAL EXCITATIONS OF GRAPHYNE

The DFT and QP band structures are presented in Fig. 1(b), respectively. Because of the depressed screening in such a 2D semiconductor, enhanced self-energy correction enlarges the band gap from the DFT predicted 0.43 eV to 1.4 eV, showing an enhanced many-electron correction that is also observed in other 2D semiconductors.[5,29] At the same time, the direct band gap is kept at the M point even after the GW correction.

The optical absorption spectra of graphyne are presented in Fig. 2(a). In the single-particle absorption spectrum without e-h interactions included (the blue curve), the optical absorption edge starts from the QP band gap (∼1.4 eV) due to the direct-gap nature. More interestingly, a huge optical absorbance is observed. For example, within the near-infrared and visible frequency regime, more than 6% of the incident light will be absorbed by a single atomic layer, making our

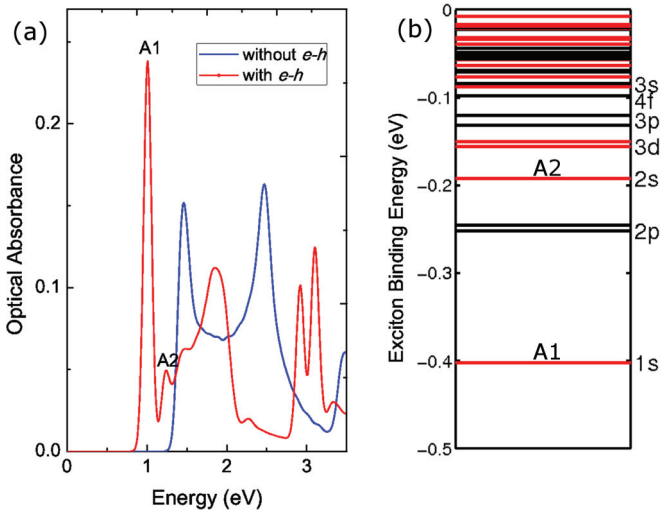

FIG. 2. (Color online) (a) Optical absorption spectra of graphyne with and without e-h interaction included. The absorbance value is obtained according to Ref. 37. A 0.05 eV Gaussian broadening is applied to obtain these optical absorption spectra. (b) Excitonic spectra of bound excitons. The black lines represent dark states and those red lines represent bright excitons.

studied graphyne to be one of the most efficient optical absorbers. This huge optical absorbance is from the significant overlap between the valence and conduction π electronic states in such a confined structure and consequently enhanced dipole transitions.[37]

After including e-h interactions, we observe dramatic excitonic effects on the optical absorption spectrum as shown in Fig. 2(a) (the red curve). First, two new absorption peaks (A1 and A2) appear below the QP band gap because of the formation of e-h pairs (excitons). In particular, the most prominent exciton with the lowest energy is located at 1.0 eV, implying a 0.4-eV e-h binding energy, which is an order of magnitude larger than those of excitons in bulk semiconductors. These enhanced excitonic effects are due to the substantially depressed screening and quantum confinement.[1,3,5]

Moreover, we have calculated the spin-triplet excitons that are usually dark in the single-photon optical absorption spectrum due to the selection rule. The lowest-energy spin-triplet exciton is located at 0.85 eV in the optical spectrum, which is 150 meV below the first bright singlet exciton (A1) that is located at 1 eV. Such an enhanced spin singlet-triplet splitting (∼150 meV) is around an order of magnitude larger than those of typical semiconductors and even carbon nanotubes.[38] Since the spin singlet-triplet splitting is decided by the e-h exchange interaction,[37] the tremendous one observed in graphyne is from the significant overlap of electron and hole wave functions, which is consistent with the aforementioned huge optical absorbance.

The above unique optical properties of graphyne may give hope to numerous potential applications. For example, the strongly bright exciton A1 located at 1.0 eV,[39] the significant e-h binding energy (∼400 meV) and impressive spin singlet-triplet splitting give hope to potential PV materials.[40,41] Other than energy applications, our studied graphyne structure

exhibits an extremely strong absorbance between 1 and 2 eV, which may be of interest for biomedical applications.[42] It has to be pointed out that we only predict the fundamental properties of graphyne. For realistic applications, many other factors, such as electron-phonon interactions, defects, and mobility, will be crucial.

IV. EXCITON SPECTRUM OF GRAPHYNE

Beyond focusing on these optically prominent excitons, it is necessary to study the whole exciton spectrum, which is crucial to understand *e-h* interactions and subsequent modeling efforts. In Fig. 2(b) we list all bound exciton states of graphyne according to their binding energy. Because the direct band gap is located at M points of the first BZ, each exciton energy level is actually triple degenerated, but here we only consider one set of them. An immediate question is raised from Fig. 2(b); the second lowest energy levels are doubly degenerated and dark in the optical absorption spectrum. This substantially conflicts the usual hydrogenic exciton model, in which the lowest two excitons shall be the nondegenerated and bright $1s$ and $2s$ states, respectively.

In order to understand this unusual exciton spectrum, we first focus on their real-space wave functions. In Fig. 3 the six lowest-energy excitonic states are plotted (for degenerated states, we only plot one of them). We see the distributions of wave functions are similar to the hydrogenic model, e.g., the spherical symmetry of the s orbital, those angular momentum characters of p, d, and f orbitals, and their nodal structures. As a result, we identify these states with the same parities as the hydrogenic model, i.e., $1s$, $2s$, and $2p$, etc., as marked in Fig. 2(b). The optical selection rules on these states are also almost preserved. For example the s states are bright while the p states are dark. The only exception is the $3d$ states, which shall be dark while they are slightly bright in Fig. 2(b). This is due to the fact that the calculated graphyne structure is only quasi-2D, which cannot keep the perfect symmetry.

On the other hand, the order of these exciton states in Fig. 2(b) is $1s$, $2p$, $2s$, $3d$, $3p$, and $4f$, etc., which is qualitatively different from exciton spectra of either the 2D or 3D hydrogenic model. Moreover, if we fit the energy dependence of those bright s states according to the main quantum number n, the first-principles result decays much more slowly than the $\frac{1}{(n-0.5)^2}$ relation of the 2D hydrogenic model or the $\frac{1}{n^2}$ relation of the 3D hydrogenic model. These similarities and dissimilarities between *ab initio* results and hydrogenic models encourage us to modify the hydrogenic model by approximating the perpendicular confinement.

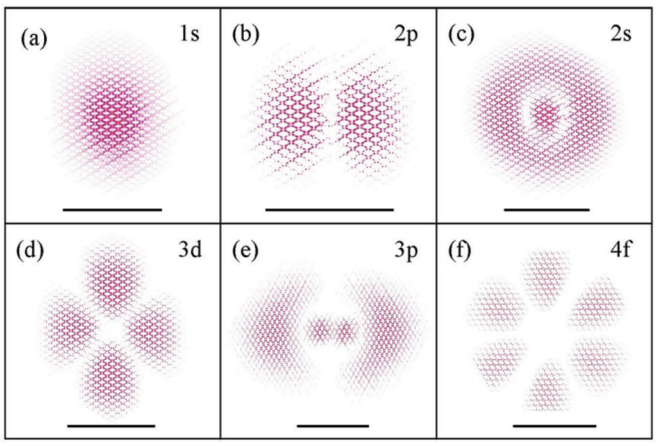

FIG. 3. (Color online) Top views of the square of the electron wave functions of the characteristic bound excitons of graphyne from Fig. 2(b). The hole is fixed at the center of each plot. The real-space 10-nm scale bars are presented, respectively.

V. AN EXCITON MODEL IN 2D SEMICONDUCTORS

An obvious improvement to the typical 3D hydrogenic model is to confine the Coulomb interaction within a finite width perpendicular to the graphyne layer. In particular, the typical size of excitons shown in Fig. 3 is around 10 nm, which is much larger than the thickness of the electron distribution perpendicular to the graphyne plane ($\sim$ a few Å). This validates the first-order approximation that the thickness of graphyne is a small number compared to the average distance between electron and hole. As a result, we introduce the following modified Coulomb interaction:

$$V(r) = -\frac{1}{\varepsilon_0}\frac{1}{\sqrt{r^2 + d_0^2}}, \tag{1}$$

where r is the polar radius of cylindrical coordinates and d_0 is the parameter to reflect the effective thickness of 2D excitons. Actually this type of Coulomb interaction had been applied to study many-electron systems before.[43–45] With the help of the separation of variables, all exciton levels can be obtained by solving a 1D single-particle Schrodinger equation [Eq. (2), in Hartree atomic units] by the finite-element simulation,

$$\left[\frac{1}{2m^*}\left(-\frac{d^2}{dr^2} - \frac{1}{r}\frac{d}{dr} + \frac{l^2}{r^2}\right) - \frac{1}{\sqrt{r^2 + d_0^2}}\right] \cdot R(r) = E \cdot R(r). \tag{2}$$

The effective mass m^* is the reduced mass of electrons and holes (averaged by all in-plane directions), which can be obtained by simple DFT calculations because many-electron corrections usually do not change the curvature of electronic bands significantly. In a word, only one parameter, the effective thickness d_0, is essential in this model.

In realistic cases, we optimize d_0 according to the energy spacing between the first two bright singlet excitonic ($1s$ and $2s$) states, which shall be the easiest data from the optical absorption or luminescence spectrum experiments. In this work, as an example, we fit d_0 according to the energy spacing of $1s$ and $2s$ states from the *ab initio* simulated optical absorption spectrum shown in Fig. 2(a) (A_1 and A_2). The results are concluded in Fig. 4, in which this modified hydrogenic model provides surprisingly good explanations. The deviation of the binding energy between the model and *ab initio* result is less than 40 meV. Considering the extremely light simulation of the model, this model shall be of help for researchers who are not experts of the first-principles MBPT. Besides the binding energies, the eigenstates of the model exhibit exactly the same energy order as the results from *ab initio* simulation.

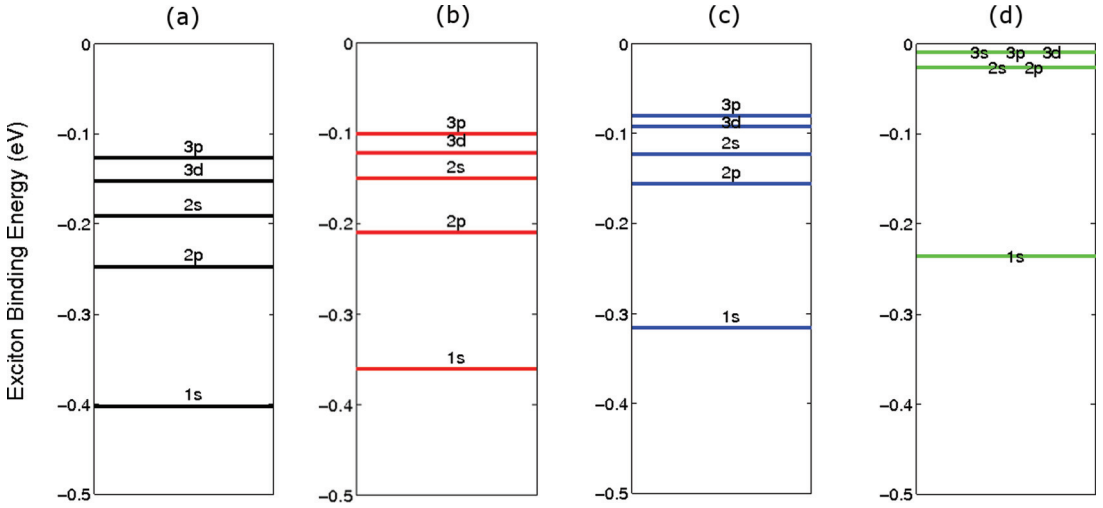

FIG. 4. (Color online) Exciton spectra. (a), (b), (c), and (d) are results of graphyne from the *ab initio* simulation, our model ($m^* = 0.071m_0, d_0 = 2.44$ nm), the model from Ref. 46, and the original 2D hydrogenic model, respectively.

In Fig. 5, we have presented the wave functions of those excitonic states solved from Eq. (2), using the parameter of graphyne. More surprisingly, this model even gives the similarly sized wave functions of these excitons (∼10 nm) compared to those first-principles results, in addition to the same nodal structures.

We have compared our results with another recently proposed model for describing *e-h* interactions with negligible exchange interactions in 2D semiconductors[46,47] in Fig. 4(c). This model also gives reasonably good predictions; the *e-h* binding energy is around 320 meV, around 80 meV less than the *ab initio* result. As shown in Fig. 4, our model provides different results. This is not surprising because our model has a fitted parameter d_0 while the model from Ref. 46 does not have tunable parameters. In particular, d_0 is fitted from singlet states and it thus more aptly includes subtle many-electron effects, such as *e-h* exchange interactions. This brings new physical meanings to the parameter d_0 in addition to the thickness effect. Further discussion will be presented in Sec. VII.

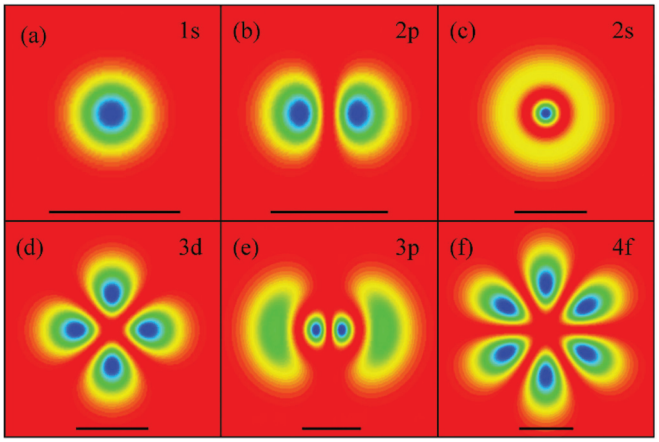

FIG. 5. (Color online) Top views of the square of the electron wave functions of the characteristic bound excitons of graphyne solved by our model. The hole is fixed at the center of each plot. The real-space 10-nm scale bars are presented, respectively.

VI. APPLICATION OF THE EXCITON MODEL TO GRAPHANE

Meanwhile, we also calculate excitonic spectra of another important 2D graphene derivative, hydrogen-passivated graphene (graphane). Here the lowest-energy exciton of graphane is a charge-transfer and relatively dark one,[15] which is qualitatively different from the bright and non-charge-transfer exciton in graphyne. This difference provides us a good opportunity to justify the application range of our model. The results are concluded in Fig. 6. We again obtain the excellent consistence between exciton spectra from both the model and *ab initio* simulation. For the comparison purpose, we have listed the results from the original 2D hydrogenic model, which exhibit substantially larger errors for both graphyne and graphane: The binding energy is much smaller than that from *ab initio* simulations; the degeneracy of excitons is not correct and the order of exciton energy levels are qualitatively wrong.

We have compared our results with the previous model[46] as well. Because of the lack of exchange interactions due to the charge-transfer nature of involved excitons, all models give the similar result about the binding energy of excitons in graphane, around 160 meV, which agrees well with the *ab initio* result.

VII. FURTHER DISCUSSION OF THE EXCITON MODEL

Our model can provide more systematic knowledge of excitons in 2D semiconductors. We have plotted the potential profiles of bare Coulomb potential and our modified *e-h* interaction potential in Fig. 7(a). They are significantly different from each other when r is small, e.g., r is less than 2 Å. This tells us the most significant corrections from our model are for those smaller-sized exciton states. Furthermore, we have presented how the binding energy of the first three s exciton states evolves with effective thickness (d_0) from the solution of Eq. (2), where the effective mass $m^* = m_0$ (for other m^* values, the binding energy and effective thickness can be scaled by m^*, respectively), in Fig. 7(b). This shows the quantum confinement effects on *e-h* pairs. For example,

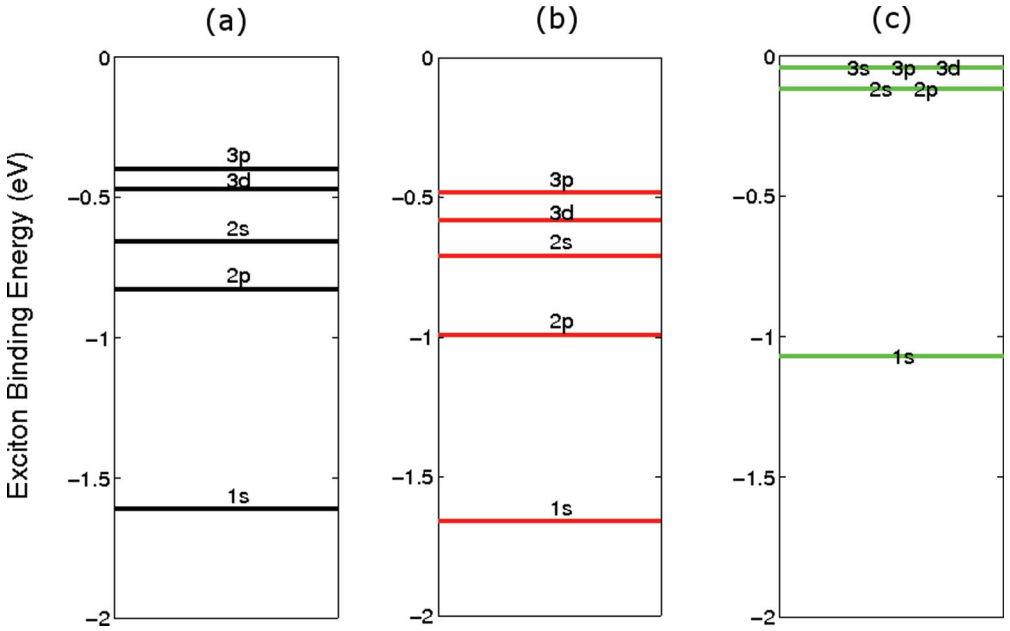

FIG. 6. (Color online) Exciton spectra. (a), (b), and (c) are results of graphane from the *ab initio* simulation, our model ($m^* = 0.353m_0, d_0 =$ 0.54 nm), and the original 2D hydrogenic model, respectively.

we can see the energy spacings between these s states shrink as we increase d_0. This explains why graphyne and graphane have a slower decaying trend of the exciton binding energy than that of the original 2D hydrogenic model. Finally, it has to be pointed out that our model only works well with 2D semiconductors with the direct band gap, whose effective masses of electrons and holes are not extremely anisotropic.

It is prudent to identify additional physical mechanisms that are tied to the fitted parameter d_0, which was originally introduced as the finite thickness of these 2D semiconductors. This interpretation of d_0 works well for charge-transfer excitons in graphane, whose e-h exchange interaction is negligible. However, we find that d_0 is around 2.44 nm in graphyne, which is too large to be regarded as the effective thickness. This is partially due to the fact that our model in Eq. (2) does not include the e-h exchange interaction explicitly. In order to specify the role of e-h exchange interactions, we apply this model to fit the triplet exciton binding energy spectrum of graphyne, as shown in Fig. 8. Our model results agree very well with the *ab initio* GW-BSE simulation and the fitted parameter d_0 is around 1.4 nm, which is significantly smaller than that of singlet states. However this d_0 is still too large to be interpreted as the physical thickness of graphyne. This is not strange because electrons and holes are not spatially separated in graphyne and, consequently, the fitted d_0 is an averaged result. Therefore, other than the thickness, it would be better to generally treat d_0 as a fitting parameter that

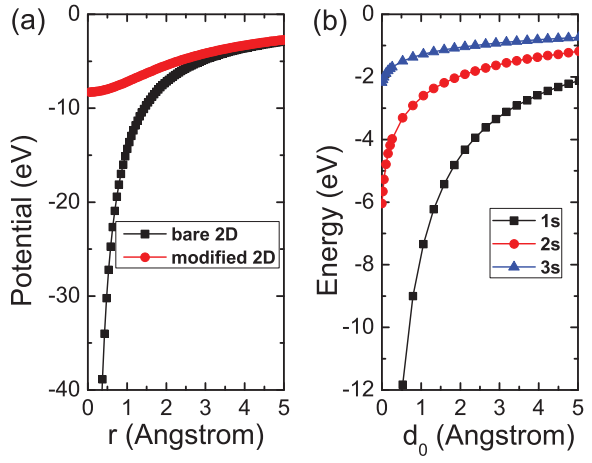

FIG. 7. (Color online) (a) Bare Coulomb potential and our modified potential for e-h interactions. (b) The evolution of the binding energy of 1s, 2s, and 3s states according to the effective thickness d_0 from the solution of Eq. (2) when $m^* = m_0$.

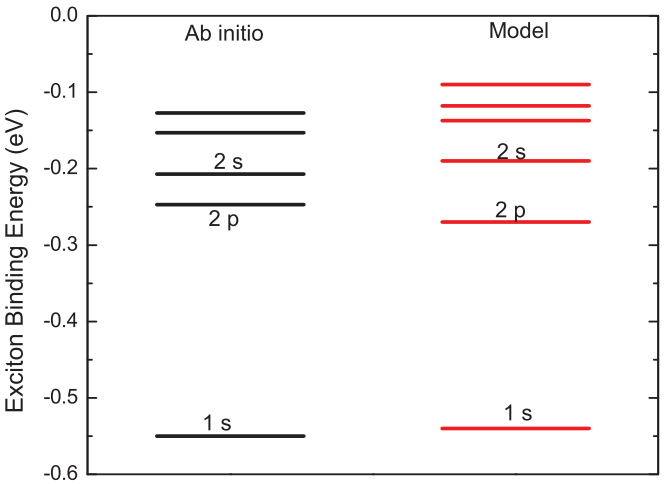

FIG. 8. (Color online) Triplet exciton binding energy spectra from the *ab initio* simulation (black lines) and our model (red lines) with $d_0 = 1.4$ nm, respectively.

approximately includes the thickness confinement as well as other many-electron effects.

VIII. CONCLUSIONS

In conclusion, we perform the first-principle GW-BSE approach to study optical excitations of graphyne. Our calculation reveals that graphyne is a promising material which may own the potential for a wide range of applications, e.g., PV and photo therapy. These quantitative predictions shall be of importance to spur more research resources and interest to graphyne. At the same time, we analyze the excitonic spectra of graphyne and propose a modified hydrogenic model that not only explains the exciton spectrum of graphyne but also that of graphane, shedding light on a convenient approach to understanding excitonic spectra and estimating the binding energy of excitons in the 2D semiconductor.

ACKNOWLEDGMENTS

This research is supported by NSF Grant No. DMR-1207141. The computational resources have been provided by Lonestar of Teragrid at the Texas Advanced Computing Center. The ground state calculation is performed by QUANTUM ESPRESSO.[48] The GW-BSE calculation is done with the BERKELEYGW package.[49]

[1] C. D. Spataru, S. Ismail-Beigi, L. X. Benedict, and S. G. Louie, Phys. Rev. Lett. **92**, 077402 (2004).
[2] F. Wang, G. Dukovic, L. E. Brus, and T. F. Heinz, Science **308**, 838 (2005).
[3] G. D. Scholes and G. Rumbles, Nat. Mater. **5**, 683 (2006).
[4] Z. Wang, H. Pedrosa, T. Krauss, and L. Rothberg, Phys. Rev. Lett. **96**, 047403 (2006).
[5] L. Wirtz, A. Marini, and A. Rubio, Phys. Rev. Lett. **96**, 126104 (2006).
[6] L. Yang, J. Deslippe, C.-H. Park, M. L. Cohen, and S. G. Louie, Phys. Rev. Lett. **103**, 186802 (2009).
[7] V. Perebeinos, J. Tersoff, and P. Avouris, Phys. Rev. Lett. **92**, 257402 (2004).
[8] T. Ando, J. Phys. Soc. Jpn. **66**, 1066 (1997).
[9] R. Rinaldi *et al.*, Phys. Rev. Lett. **73**, 2899 (1994).
[10] R. C. Miller, D. A. Kleinman, W. T. Tsang, and A. C. Gossard, Phys. Rev. B **24**, 1134 (1981).
[11] G. Bastard, E. E. Mendez, L. L. Chang, and L. Esaki, Phys. Rev. B **26**, 1974 (1982).
[12] R. L. Greene, K. K. Bajaj, and D. E. Phelps, Phys. Rev. B **29**, 1807 (1984).
[13] L. C. Andreani and A. Pasquarello, Phys. Rev. B **42**, 8928 (1990).
[14] H. Mathieu, P. Lefebvre, and P. Christol, J. Appl. Phys. **72**, 300 (1992).
[15] P. Cudazzo, C. Attacalite, I. V. Tokatly, and A. Rubio, Phys. Rev. Lett. **104**, 226804 (2010).
[16] K. F. Mak, J. Shan, and T. F. Heinz, Phys. Rev. Lett. **106**, 046401 (2011).
[17] Duminda K. Samarakoon, Zhifan Chen, Chantel Nicolas, and Xiao-Qian Wang, Small **7**, 965 (2011)
[18] S. Lebègue, M. Klintenberg, O. Eriksson, and M. I. Katsnelson, Phys. Rev. B **79**, 245117 (2009).
[19] R. H. Baughman, H. Eckhardt, and M. Kertesz, J. Chem. Phys. **87**, 6687 (1987).
[20] N. Narita, S. Nagai, S. Suzuki, and K. Nakao, Phys. Rev. B **58**, 11009 (1998).
[21] J. Zhou, K. Lv, Q. Wang, X. S. Chen, Q. Sun, and P. Jena, J. Chem. Phys. **134**, 174701 (2011).
[22] J. Kang, J. Li, F. Wu, S. Li, and J. Xia, J. Phys. Chem. C **115**, 20466 (2011).
[23] K. Srinivasu and S. K. Ghosh, J. Phys. Chem. C **116**, 5951 (2012).
[24] D. Malko, C. Neiss, F. Viñes, and A. Görling, Phys. Rev. Lett. **108**, 086804 (2012).
[25] J. O. Sofo, A. S. Chaudhari, and G. D. Barber, Phys. Rev. B **75**, 153401 (2007).
[26] D. C. Elias *et al.*, Science **323**, 610 (2009).
[27] M. Z. S. Flores, P. A. S. Autreto, S. B. Legoas, and D. S. Galvao, Nanotechnology **20**, 465704 (2009).
[28] O. Leenaerts, H. Peelaers, A. D. Hernández-Nieves, B. Partoens, and F. M. Peeters, Phys. Rev. B **82**, 195436 (2010).
[29] G. Luo *et al.*, Phys. Rev. B **84**, 075439 (2011).
[30] J. M. Kehoe *et al.*, Org. Lett. **2**, 969 (2000).
[31] W. B. Wan and M. M. Haley, J. Org. Chem. **66**, 3893 (2001).
[32] J. A. Marsden, G. J. Palmer, and M. M. Haley, Eur. J. Org. Chem. **2003**, 2355 (2003).
[33] M. M. Haley, Pure Appl. Chem. **80**, 519 (2008).
[34] F. Diederich and M. Kivala, Adv. Mater. **22**, 803 (2010).
[35] A. Hirsch, Nat. Mater. **9**, 868 (2010).
[36] M. S. Hybertsen and S. G. Louie, Phys. Rev. B **34**, 5390 (1986).
[37] M. Rohlfing and S. G. Louie, Phys. Rev. B **62**, 4927 (2000).
[38] V. Perebeinos, J. Tersoff, and P. Avouris, Nano. Lett. **5**, 2495 (2005).
[39] W. Shockley and H. J. Queisser, J. Appl. Phys. **32**, 510 (1961).
[40] J. Peet *et al.*, Nat. Mater. **6**, 497 (2007).
[41] S. H. Park *et al.*, Nat. Photon. **3**, 297 (2009).
[42] C. M. Hessel, V. P. Pattani, M. Rasch, M. G. Panthani, B. Koo, J. W. Tunnell, and B. A. Korgel, Nano. Lett. **11**, 2560 (2011).
[43] Y. E. Lozovik, I. V. Ovchinnikov, S. Y. Volkov, L. V. Butov, and D. S. Chemla, Phys. Rev. B **65**, 235304 (2002).
[44] M. Y. J. Tan, N. D. Drummond, and R. J. Needs, Phys. Rev. B **71**, 033303 (2005).
[45] C. Schindler and R. Zimmermann, Phys. Rev. B **78**, 045313 (2008).
[46] P. Cudazzo, I. V. Tokatly, and A. Rubio, Phys. Rev. B **84**, 085406 (2011).
[47] L. V. Keldysh, JETP Lett. **29**, 658 (1979).
[48] P. Giannozzi *et al.*, J. Phys.: Condens. Matter **21**, 395502 (2009).
[49] J. Deslippe *et al.*, Comput. Phys. Commun. **183**, 1269 (2012).